

Supplementary Information for:

Mie-Coupled Bound Guided States in Nanowire Geometric Superlattices

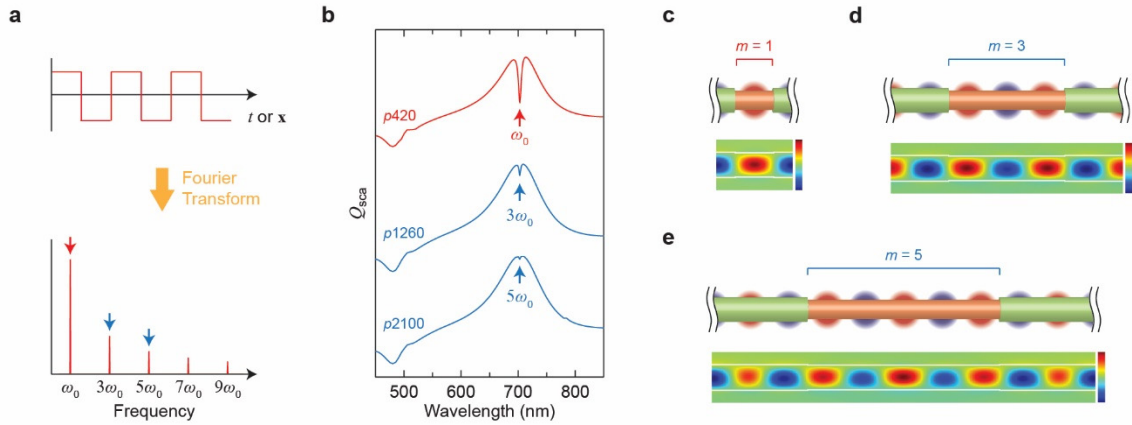
Seokhyoung Kim¹, Kyoung-Ho Kim^{1,2}, David J. Hill¹, Hong-Gyu Park^{2}, and James F. Cahoon^{1*}*

Supplementary Information includes:

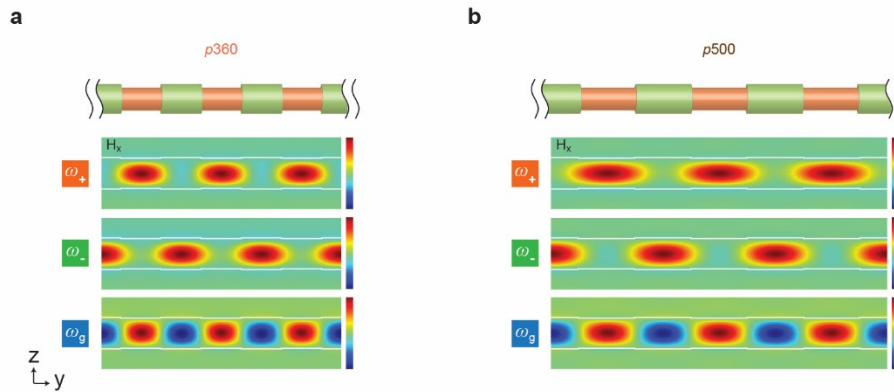
Supplementary Figures 1-11

Supplementary Tables 1-2

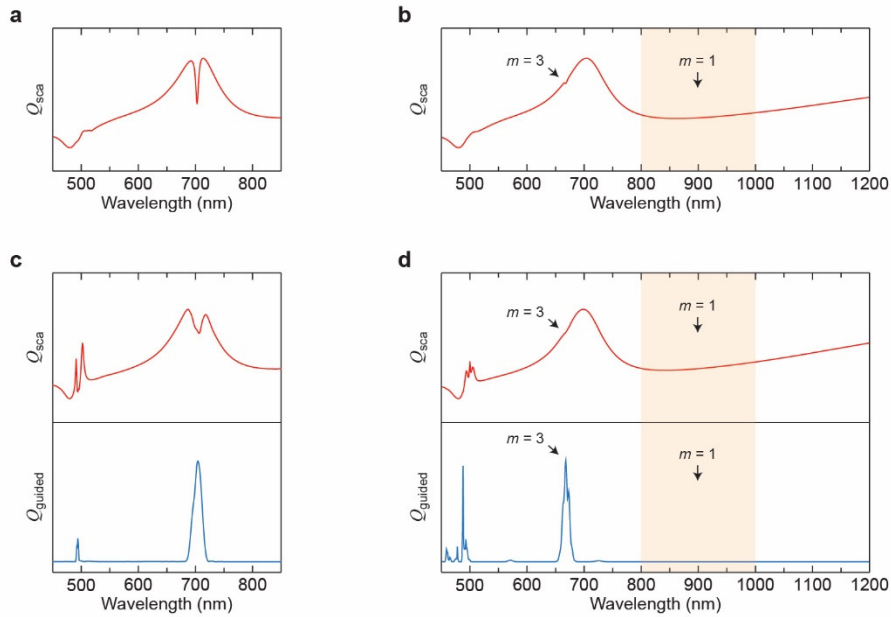
Supplementary Movie 1-4 captions



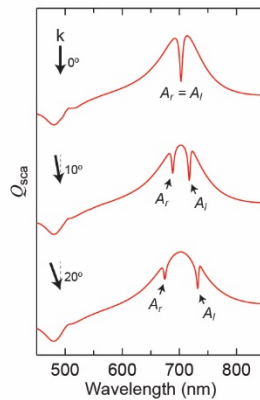
Supplementary Figure 1 | Fourier selection of BGS by higher harmonics. **a**, A square wave representing a GSL structure and its Fourier series that consists of odd-numbered harmonics of the fundamental frequency. **b**, Q_{sca} spectrum of NW GSLs with $d = 140$ nm and $e = 135$ nm of three different values of $p = 420$ nm (top), $p = 1260$ nm (middle) and $p = 2100$ nm (bottom). Pitch was varied to tailor higher harmonic interactions with a Mie resonance fixed at the same wavelength. **c-e**, Schematic and calculated magnetic field profiles for the GSLs in panel b at the dip, showing a BGS mode with $m = 1$ (**c**), $m = 3$ (**d**) and $m = 5$ (**e**) antinodes confined at each segment.



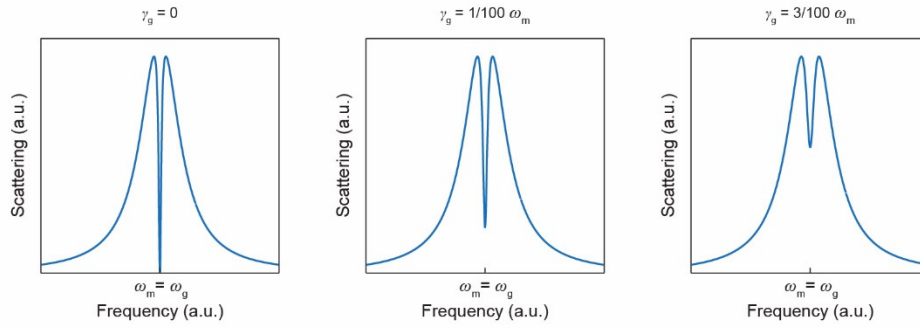
Supplementary Figure 2 | Calculated Magnetic Field Profiles of a GSL with varying pitch. **a-b**, Schematic and calculated magnetic field profiles for a GSL with $p = 360$ nm (**a**) and $p = 500$ nm (**b**) from Figure 1c, showing coupled TM_{11} dipolar modes appearing in small diameter regions (ω_+ , top) and large diameter regions (ω_- , middle), and a standing wave as a superposition of counter-propagating HE_{11} guided modes (ω_g , bottom).



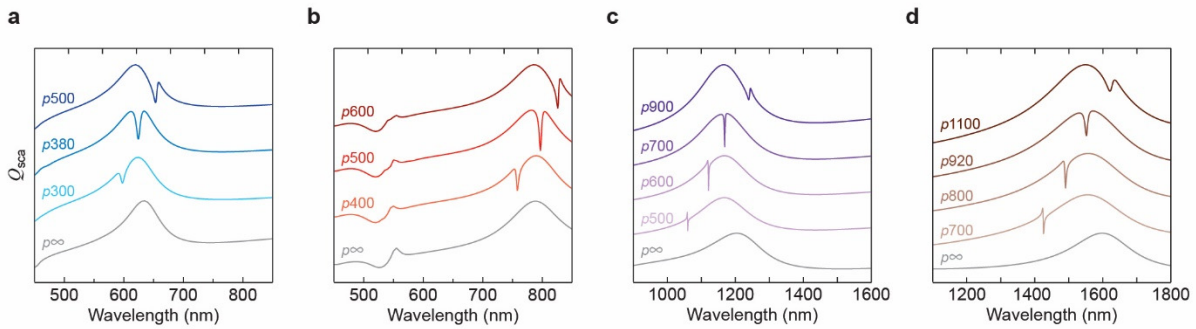
Supplementary Figure 3 | Disappearance of BGS coupling at long pitch values outside the Mie resonance envelope. **a-b**, Simulated Q_{sca} spectra with $d = 140$ nm and $e = 135$ nm for an on-resonance $p = 420$ nm (**a**) and an off-resonance $p = 1000$ nm (**b**) NW GSL under plane wave illumination. A scattering dip is not observed for $p = 1000$ nm in the shaded region of the spectrum where the first-order ($m = 1$) BGS is expected, but the third-order ($m = 3$) mode appears at ~ 668 nm. **c-d**, Simulated Q_{sca} spectra (upper graphs) and Q_{guided} spectra (lower graphs) for an on-resonance $p = 420$ nm (**c**) and an off-resonance $p = 1000$ nm (**d**) GSL-WG under illumination with a Gaussian beam. For the off-resonance structure (panel **d**), no guided power is observed in the shaded region of the spectrum where the first-order ($m = 1$) BGS is expected, but guided power from the third-order ($m = 3$) mode appears at ~ 668 nm.



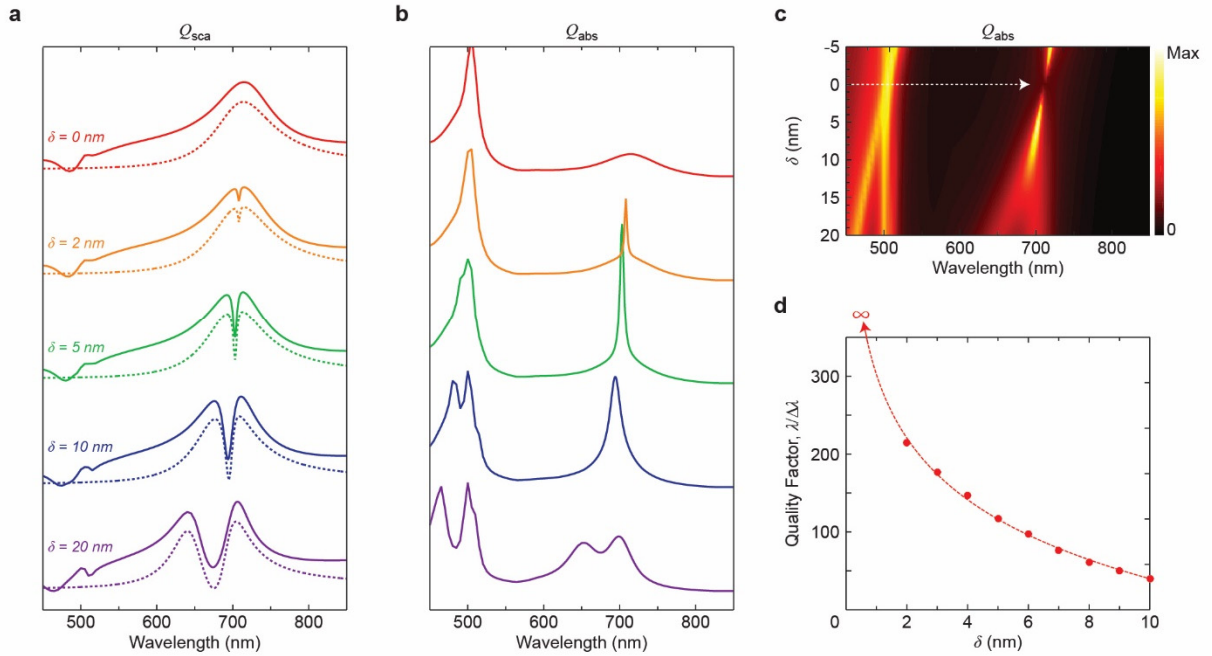
Supplementary Figure 4 | Incident angle dependence of BGS coupling. Simulated Q_{sca} spectra of a NW GSL with $d = 140$ nm, $e = 135$ nm, and $p = 420$ nm under plane wave illumination at 0° (upper), 10° (middle), and 20° (bottom) with respect to the normal, showing a splitting of the BGS into primarily right-propagating (A_r) and left-propagating (A_l) BGS modes.



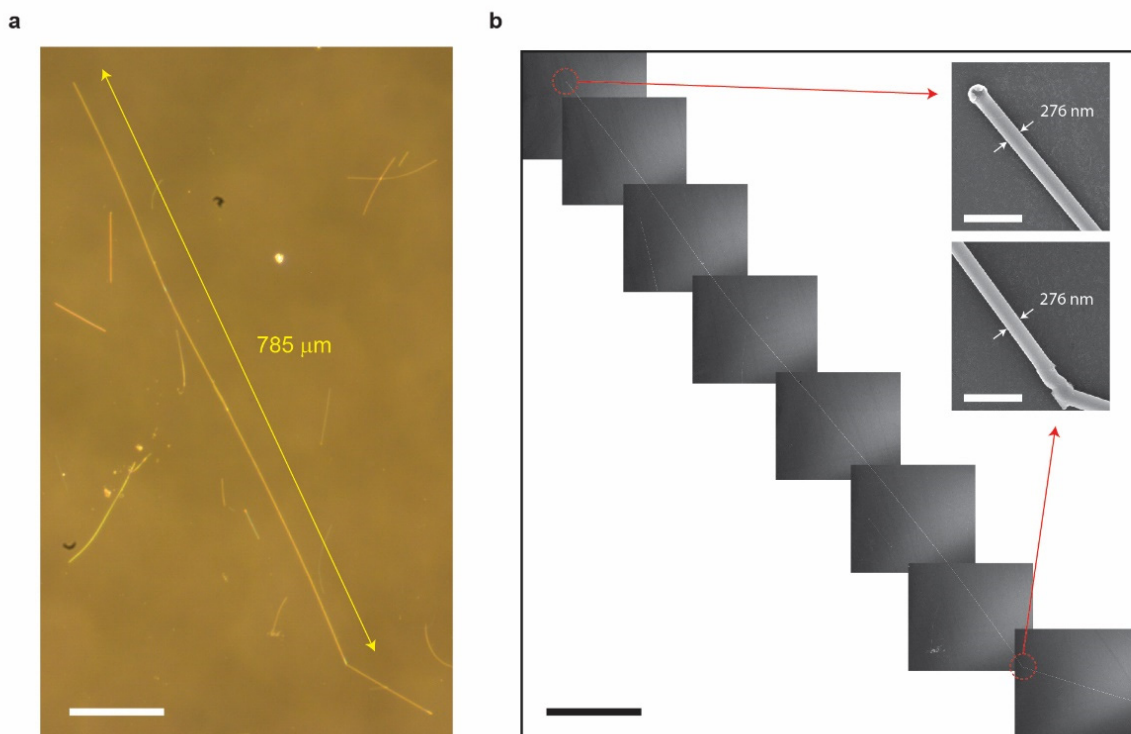
Supplementary Figure 5 | Schematic plots of Mie-BGS coupling with and without γ_g . Schematic scattering plots for $\omega_m = \omega_g$ when γ_g is zero (left), $1/100 \omega_m$ (middle) and $3/100 \omega_m$ (right).



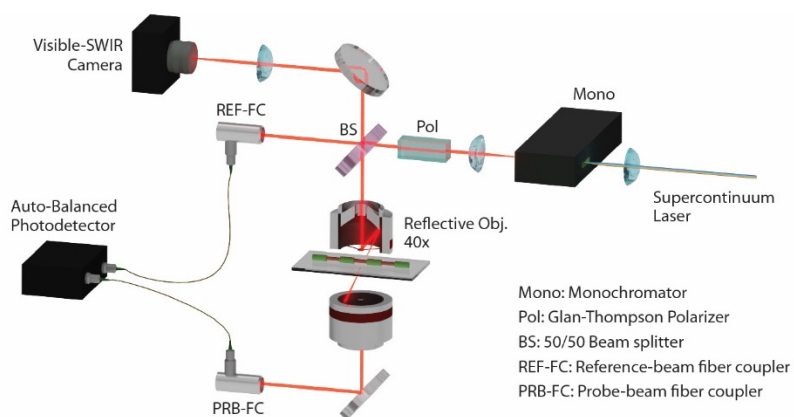
Supplementary Figure 6 | Diameter dependence and spectral tunability of Mie-BGS coupling. Simulated Q_{sca} spectra of GSLs of selected pitches with $d = 120$ nm, $e = 115$ nm (a), $d = 160$ nm, $e = 155$ nm (b), $d = 250$ nm, $e = 245$ nm (c), and $d = 340$ nm, $e = 330$ nm (d).



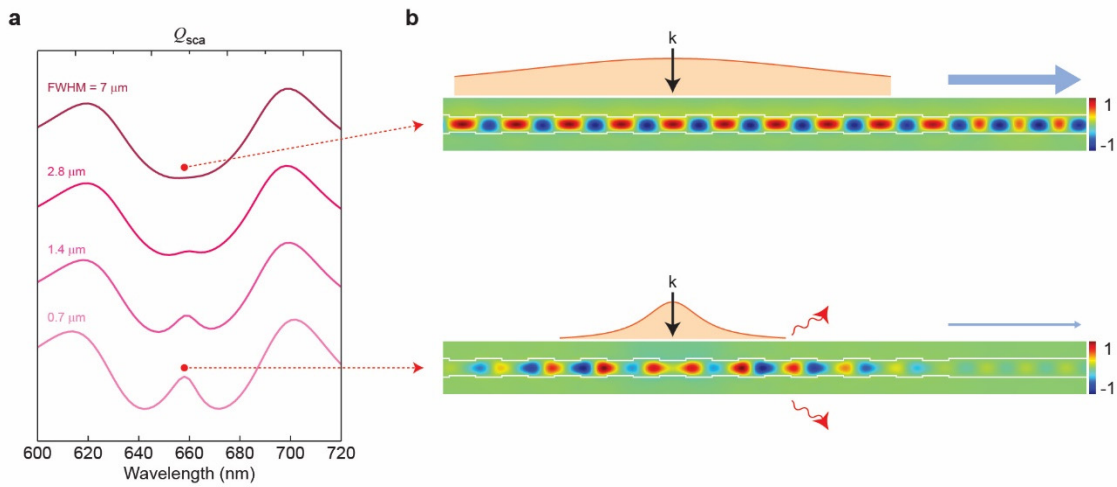
Supplementary Figure 7 | Effect of modulation depth on bound character of the BGS. a, Numerically calculated Q_{sca} spectra (solid lines) and analytical fit by TCMT (dotted lines) for a NW GSL with $d=140$ nm, $p=420$ nm and varying δ of 0, 2, 5, 10, and 20 nm. $\delta=0$ nm corresponds to a NW with uniform diameter. Parameters for TCMT spectra are provided in Table S2. **b,** Numerically calculated Q_{abs} spectra of GSLs from panel a, showing a broad background peak for $\delta=0$ nm and appearance of a high-quality factor absorption peak for non-zero δ that eventually bifurcates into two peaks at $\delta > 15$ nm. **c,** Two-dimensional Q_{sca} heat map with vertical and horizontal axes for δ and wavelength, respectively, showing a vanishing point at $\delta=0$ nm that corresponds to a completely bound guided state (BGS). **d,** Quality factor ($\lambda/\Delta\lambda$) calculated from the fit parameters (Supplementary Table 2) used panel b plotted against δ , which extrapolates to infinity as δ approaches zero.



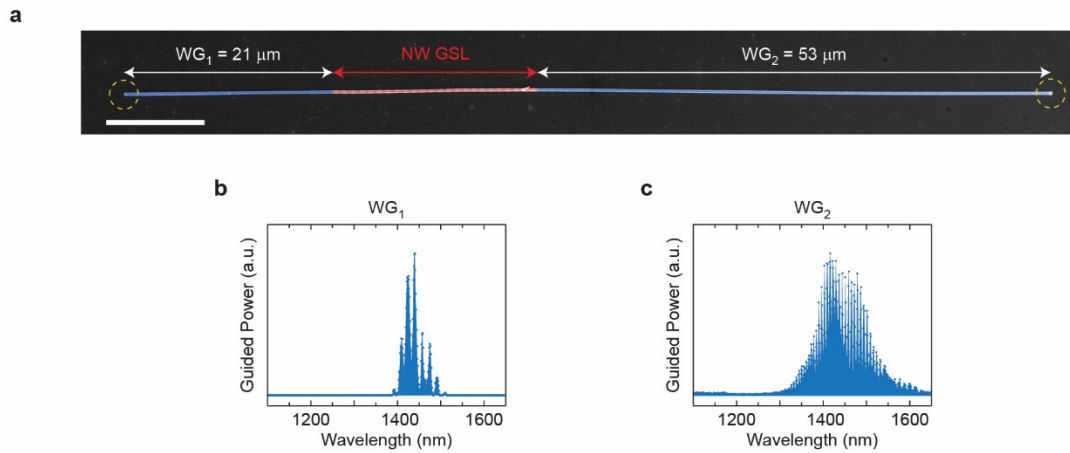
Supplementary Figure 8 | NW with length of nearly 1 mm with no variation in diameter. a-b, Optical (a) and SEM (b) images of a NW exhibiting no diameter variation over nearly 1 mm; scale bars, 100 μm . Insets: Magnified views at each end of a straight portion of the NW; scale bars, 1 μm .



Supplementary Figure 9 | Instrumental setup. Laser microscope for polarization-resolved bright-field extinction measurements.



Supplementary Figure 10 | Effect of Gaussian beam width. **a**, Q_{sca} spectra around the scattering dip region of a GSL with $d = 140$ nm, $e = 115$ nm and $p = 400$ nm under focused Gaussian illumination of varying width. Each spectrum is labeled with its Gaussian full-width at half maximum. Absorptive loss is artificially turned off to only account for scattering characteristics. **b**, Calculated magnetic field snapshots at marked locations from panel **a** and Supplementary Movie 3-4, showing coherent coupling to the BGS under a large beam (top) and radiative loss under a small beam (bottom).



Supplementary Figure 11 | Fabry-Perot cavity free spectral ranges in WGs of different lengths. **a**, A NW GSL attached to WGs at both ends in lengths of 21 and 53 μm ; scale bar, 10 μm . **b-c**, Experimental guided spectra collected from WG₁ (**b**) and WG₂ (**c**).

Supplementary Table 1 | Parameters used in the TCMT for fitting Q_{sca} spectra in Figure 1c

	λ_m (nm)	λ_g (nm)	ω_m (THz)	ω_g (THz)	ω_c (THz)	γ_m (THz)	γ_g (THz)
p^∞	700	1000	2691	1884	- ^a	177	- ^a
$p360$	700	680	2691	2770	24	179	5.4
$p420$	700	703	2691	2679	30	179	5.4
$p500$	700	726	2691	2595	30	179	4.5

^a Any arbitrary value can be chosen.

Supplementary Table 2 | Parameters used in the TCMT for fitting Q_{sca} spectra in Supplementary Figure 7

δ (nm)	λ_m (nm)	λ_g (nm)	ω_m (THz)	ω_g (THz)	ω_c (THz)	γ_m (THz)	γ_g (THz)
0	711	- ^a	- ^a	- ^a	0	177	- ^a
2	707	708	2664	2661	12	178	5.3
5	700	703	2691	2679	30	179	5.4
10	687	695	2742	2710	55	183	5.5
20	665	675	2833	2791	129	189	5.7

^a Any arbitrary value can be chosen.